New Analogues of Amonafide and Elinafide, Containing Aromatic Heterocycles: Synthesis, Antitumor Activity, Molecular Modeling, and DNA Binding Properties

Miguel F. Braña,*[,†] Mónica Cacho,[†] Mario A. García,[†] Beatriz de Pascual-Teresa,[†] Ana Ramos,[†] M. Teresa Domínguez,[‡] José M. Pozuelo,[‡] Cristina Abradelo,[§] María Fernanda Rey-Stolle,[§] Mercedes Yuste,[§] Mónica Báñez-Coronel,[||] and Juan Carlos Lacal[||]

Departamentos de Ciencias Químicas, Biología Celular, Bioquímica y Biología Molecular, Matemáticas, Física Aplicada y Fisicoquímica, Facultad de Ciencias Experimentales y de la Salud, Universidad San Pablo CEU, Urbanización Montepríncipe, 28668-Boadilla del Monte, Madrid, Spain and Instituto de Investigaciones Biomédicas, CSIC, Arturo Duperier 4, 28029-Madrid, Spain

Received May 1, 2003

Amonafide- and elinafide-related mono and bisintercalators, modified by the introduction of a π-excedent furan or thiophene ring fused to the naphthalimide moiety, have been synthesized. These compounds have shown an interesting antitumor profile. The best compound, **9**, was 2.5-fold more potent than elinafide against human colon carcinoma cells (HT-29). Molecular dynamic simulations and physicochemical experiments have demonstrated that these compounds are capable of forming stable DNA complexes. These results, together with those previously reported by us for imidazo- and pyrazinonaphthalimide analogues, have prompted us to propose that the DNA binding process does not depend on the electronic nature of the fused heterocycle.

Introduction

In our search for analogues of amonafide[1] and elinafide[2] with an improved therapeutic profile, we recently described the synthesis of new mono- and bisintercalators, where the chromophore consisted of a naphthalimide moiety, fused to an imidazole[3] or a pyrazine[4] ring. While the introduction of the imidazole did not lead to a significant improvement in biological activity, bisintercalators with activities in the order of 10^{-8} M were obtained by introduction of a π-deficient pyrazine ring. Following this study of the influence that the introduction of angular fused heterocycles to the naphthalimide moiety has on the antitumor activity, in the present article we describe the synthesis, biological activity, DNA binding properties, and molecular modeling of a new series of amonafide and elinafide analogues **1**−**12**, where a π-excedent furan or thiophene ring has been introduced in the two possible orientations. Patten et al. synthesized mono- and bisintercalators with a furonaphthalimide chromophore, but the nature of the connecting chains were different, and the compounds presented lower activity than those reported here.[5]

Results and Discussion

Chemistry. The synthesis of anhydrides **17**−**20**, from which the naphthalimides **1**−**12** were prepared, was carried out following the method outlined in Scheme 1. Thus, dimethyl homophthalate was treated with the corresponding aldehyde in the presence of NaH to yield

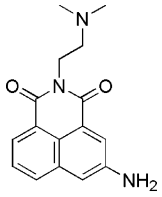

Amonafide

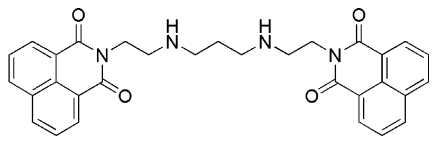

Elinafide

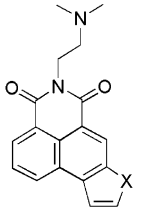

1: X = O
2: X = S

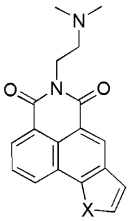

3: X = O
4: X = S

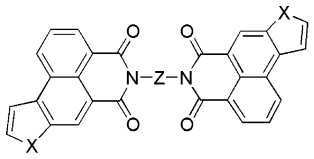

5: X = O; Z = $(CH_2)_2NH(CH_2)_3NH(CH_2)_2$
6: X = O; Z = $(CH_2)_2NCH_3(CH_2)_3NCH_3(CH_2)_2$
7: X = S; Z = $(CH_2)_2NH(CH_2)_3NH(CH_2)_2$
8: X = S; Z = $(CH_2)_2NCH_3(CH_2)_3NCH_3(CH_2)_2$

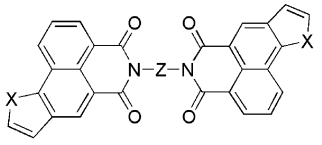

9: X = O; Z = $(CH_2)_2NH(CH_2)_3NH(CH_2)_2$
10: X = O; Z = $(CH_2)_2NCH_3(CH_2)_3NCH_3(CH_2)_2$
11: X = S; Z = $(CH_2)_2NH(CH_2)_3NH(CH_2)_2$
12: X = S; Z = $(CH_2)_2NCH_3(CH_2)_3NCH_3(CH_2)_2$

* To whom the correspondence should be addressed. Phone 34913724771; fax 34913724009; e-mail mfbrana@ceu.es.
† Departamento de Ciencias Químicas.
‡ Departamento de Biología Celular, Bioquímica y Biología Molecular.
§ Departamento de Matemáticas, Física Aplicada y Fisicoquímica.
|| Instituto de Investigaciones Biomédicas, CSIC.

10.1021/jm0308850 CCC: $27.50
Published on Web 02/07/2004

Scheme 1[a]

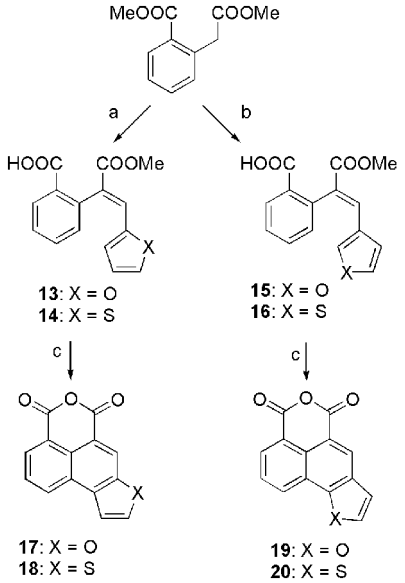

[a] Reagents: (a) for **13** 2-furanecarbaldehyde, for **14** 2-thiophenecarbaldehyde, in THF, and then NaH (80%); (b) for **15** 3-furanecarbaldehyde, for **16** 3-thiophenecarbaldehyde, in THF, and then NaH (80%); (c) (i) $I_2/h\nu$, EtOH, (ii) NaOH 1M; (iii) sat. $NaHSO_3$; (iv) Ac_2O, $\triangle$.

compounds **13**−**16**. Irradiation of these in the presence of I_2 brought about the oxidative photocyclization of the stylbene type system. The products formed were not isolated, but they were directly converted into the corresponding anhydrides **17**−**20** by hydrolysis of the ester group present in the molecule (NaOH, 1 M), followed by dehydration (Ac_2O/Δ). Furan-derived anhydrides **17** and **19** had been described previously by this method,[5] while thiophene-derived anhydrides **18** and **20** had not been obtained before.

Mononaphthalimides **1**−**4** were synthesized by treatment of the corresponding anhydride with N^1,N^1-dimethyl-1,2-ethanediamine in ethanol at reflux temperature. Bisnaphthalimides **5**−**7**, **9**, and **10** were obtained by a similar procedure, starting from the corresponding polyamine and anhydride in a 1:2 ratio. In the synthesis of **8**, **11**, and **12** an excess of amine was necessary for the reaction to be completed (TLC). However, the formation of the corresponding mononaphthalimides was not observed in the crude reaction. The synthesis of *N*,*N*′-bis(2-aminoethyl)-*N*,*N*′-dimethyl-1,3-propanediamine was carried out following the method previously described by us.[3] The rest of amines were commercially available. Compounds **1** and **5** have been reported previously.[6]

In Vitro Antiproliferative Activity. All analogues were tested for cytotoxicity against several cell lines. These include human colon carcinoma (HT-29), human cervical carcinoma (HeLa), and human prostate carcinoma (PC-3). All the compounds were tested as their methanosulfonate or hydrochloride salts.

The results are summarized in Table 1 and compared with the activity of amonafide and elinafide.

Among all the mononaphthalimides studied, compound **1**, bearing a furan ring oriented toward the *outside* of the molecule is the most active. Thus, it is 10-fold more active against HT-29, 20-fold against HeLa, and 40-fold against PC-3 than the leader compound, amonafide. However, dimerization of the chromophore, using the linker present in elinafide (compound **5**), has not resulted in an increase of activity. However this result is different from the biological data obtained for compounds **1** and **5**, in a simultaneous work carried out by Bailly et al.,[6] where the dimer proved to be over 100-times more cytotoxic against CEM leukemia cells than the monomer, with IC_{50} values of 0.6 μM and 4.9 nM, respectively. Similarly, when we carried out dimerization of the chromophore bearing the furan ring oriented toward the *inside* of the molecule (compound **9**), a remarkable increase in the antitumor potency was observed compared to the monomeric counterpart (compound **3**). Compound **9** presented $IC_{50} = 6.8$ nM against HT-29, a value that is 2.5-fold lower than the value found for elinafide under the same experimental conditions.

Table 1. Growth Inhibitory Properties for Mono- and Bisnaphthalimides **1**−**12**

	IC_{50}[a]				IC_{50}[a]		
no.	HT-29	HeLa	PC-3	no.	HT-29	HeLa	PC-3
1	0.55	0.14	0.164	**8**	0.27	0.21	1.42
2	1.15	0.80	3.50	**9**	0.0068	0.044	0.50
3	2.69	4.30	5.58	**10**	0.71	2.58	12.58
4	0.75	0.86	1.19	**11**	1.94	1.04	0.40
5	0.37	0.73	> 100	**12**	0.39	0.57	2.50
6	NT	NT	NT	amonafide	4.67	2.73	6.38
7	0.047	0.16	0.93	elinafide	0.017	0.07	0.32

[a] IC_{50}: concentration of drug (μM) to reduce cell number to 50% of control cultures.

The effect of the substitution of the oxygen atom present in the furan moiety by a sulfur atom, has been analyzed in mononaphthalimides **2** and **4**, and bisnaphthalimides **7**, **8**, **11**, and **12**. These compounds present also an interesting biological activity, but they show a different pattern of behavior than their furan counterparts. In this case, dimerization of the isomeric chromophore that bears the sulfur atom oriented toward the *outside* of the molecule resulted in a compound (**7**) which was 25-fold more active against HT-29 ($IC_{50} = 0.047$ μM) than the corresponding monomer (**2**). However, the activity of the monomer (**4**) and the dimer (**11**) were similar for the isomer bearing the sulfur atom oriented toward the *inside* of the molecule.

Compounds **6**, **8**, **10**, and **12** with a $(CH_2)_2NCH_3(CH_2)_3$-$NCH_3(CH_2)_2$ linker were chosen because methylation of the NH groups in related bis(indeno[1,2-*b*]-6-carboxamides)[7] and bis(9-methylphenazine-1-carboxamides)[8] led to an increase in potency compared to the unmethylated counterparts. In our case, methylation has brought about, in general, a decrease in activity. This effect has been observed previously in related bisnaphthalimides such as elinafide.[9] Compound **6** could not be evaluated, as it was not possible to obtain a stable salt, soluble enough in water to carry out the biological tests.

In Vivo Antiproliferative Activity. Compound **9** was selected for in vivo antitumor evaluation (due to its high antiproliferative activity). Tumors were induced by sc injection of HT-29 cells in the back of inmunosupressed mice (Swiss, nu/nu). The compound was administered ip, dissolved in sterile 0.9% NaCl. Control mice received an equivalent volume of vehicle alone, following an identical schedule. Treatment was initiated when the tumors reached a volume of 0.1 cm^3 and tu-

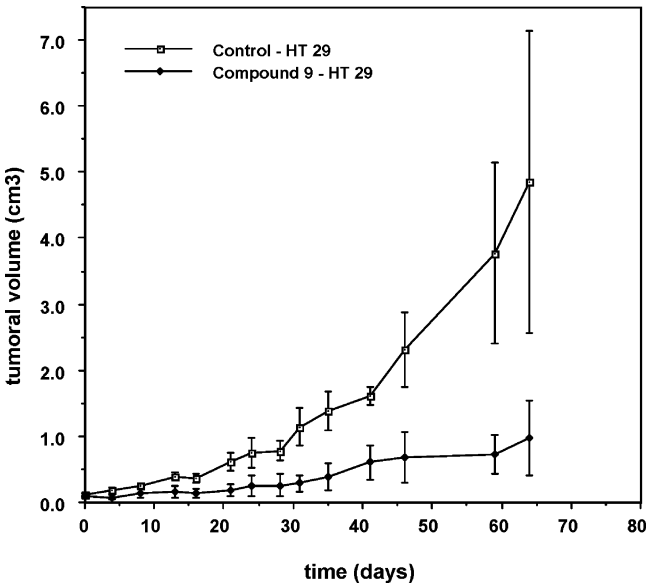

Figure 1. In vivo antitumoral activity for compound **9** on human colon cancer xenografts. Tumors were generated by sc inoculation of HT-29 cells in athymic mice. The compound (5 mg/kg) was administered ip daily for 4 consecutive days, separated by 10 days without treatment. This schedule was repeated for up to 60 days. Average tumoral volumes of treated ($n = 4$) and control mice ($n = 4$) are shown.

mors were monitored 1−2 times per week. Tumor volume was calculated using the equation $V = (Dd^2)/2$.

The result obtained for compound **9** is shown in Figure 1. Average of the tumor volume is represented for control and treated mice. The therapeutic protocol consisted of 14-days cycles, administering the compound daily for 4 consecutive days at a dose of 5 mg/kg, leaving 10 days without treatment.

This schedule caused a reduction of ∼80% of the tumoral volume at the end of the treatment, showing an in vivo antitumor effect of the compound tested.

Molecular Modeling. With the aim of rationalizing the results obtained for this new series of furonaphthalimides, a molecular modeling study was carried out for compounds **1**, **3**, **5**, and **9**. Insight into the mode of binding of compounds **1**, **3**, **5**, and **9** to DNA was gained through molecular modeling and molecular mechanics techniques using the DNA dimer $d(TG)_2$ for the monofuronaphthalimides **1** and **3** and the DNA hexamer $d(ATGCAT)_2$ for the bisfuronaphthalimides **5** and **9**. The sequence was selected according to the experimental binding preference demonstrated for this type of compounds in a NMR study[10] and to modeling experience with related intercalating agents.[3,11,12] A parallel footprinting work carried out by Bailly and co-workers[6] for compounds **1** and **5** reveals that this type of compounds exhibit and enhanced selectivity for GC rich sites if compared to elinafide.[13]

Four different model complexes were constructed for compounds **1** and **3**, by inserting the chromophores into the $d(TG)_2$ dinucleotide in the four possible orientations relative to the base pairs (Figure 2). Two through the major groove: one with the furan ring stacked between TG and the other with the furan ring stacked between AC; and the same orientations leaving the side chain in the minor groove. For dimers **5** and **9**, six different orientations were possible when binding to the DNA hexamer (Figure 3). Three with the ligand bound through the major groove and three through the minor groove. Among these three orientations, two locate the chromophores in a relative antiparallel orientation, either with the furan rings stacked between AC or between TG and the third one with a relative parallel orientation of the chromophores.

These complexes were refined and initially submitted to molecular dynamics simulations in a continuum medium of relative permittivity $4r_{ij}$ for simulating the solvent environment. Given the instability of the complexes in this environment during the simulation time, selected complexes were submitted to molecular dynamics simulations with explicit inclusion of the solvent. There is wide experience in the study of sequence-dependent structural effects in DNA and ligand−DNA complexes using this kind of methodology.[14−19]

The eight model systems initially constructed for compounds **1** and **3** were submitted to 150 ps MD simulations in water. After the equilibration period, the progression of the root-mean-square (rms) deviations of the coordinates of the solutes with respect to the initial structures was measured for all complexes and are shown in Figure 4. All four complexes simulated for compound **1**, were more stable than the corresponding simulations for compound **3**. For both compounds**,** the orientation that showed to be more stable along the simulation time was the one where the side chain remains in the major groove of the DNA dinucleotide and the furan ring is stacked between AC, which are denoted **1b** and **3b** in Figure 2. This stabilization is probably due to the fact that these orientations locate the charged amino group between N7 and O6 of the guanine base. The distances between N7 and the nitrogen proton were monitored along the simulation time, giving average values of 2.41 Å ± 0.46 and 2.34 Å ± 0.30 for **1b** and **3b**, respectively. The distances between O6 and the nitrogen proton were also monitored, giving average values of 2.84 Å ± 0.73 and 2.96 Å ± 0.54, for **1b** and **3b**, respectively. These values, together with those of the corresponding angles, indicate the presence of stable hydrogen bonds alternating between positions N7 and O6 of guanine along the simulation time. Analysis of the resulting energy-minimized average structures from the last 50 ps of the sampling time resulted in a relative stability of complex **1b** with respect to **3b**. Better stacking interactions might account for this energy difference. This result is in agreement with the biological activities reported for these compounds (Table 1).

Taking into account these results and the computer time required for this type of simulations, for compounds **5** and **9**, only the DNA complexes where these compounds are located in the major groove and in a relative antiparallel orientation of the chromophores were further submitted to molecular dynamics simulations in water. These complexes (**a** and **b** in Figure 3) were submitted to 150 ps of molecular dynamics, and the rms deviation of the complexes with respect to the initial structures were evaluated. These values remained below 2 Å for all complexes. The progression of this parameter indicates that the complexes do not experience large conformational changes during the simulation time (Figure 5). Distances and angles between the protonated

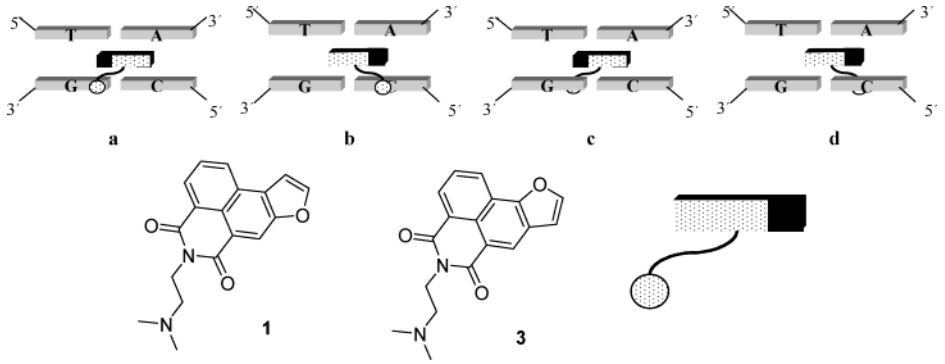

Figure 2. Schematic view from the major groove of the four complexes between compounds **1** and **3** and d(TG)$_2$. The black square in the chromophore represents the orientation of the furan ring, and the sphere represents the protonated dimethylamino group from the side chain. Left: complexes with the linker in the major groove and the furan ring stacked between TG (**a**) or between AC (**b**). Right: complexes with the linker in the minor groove and the furan ring stacked between TG (**c**) or between AC (**d**).

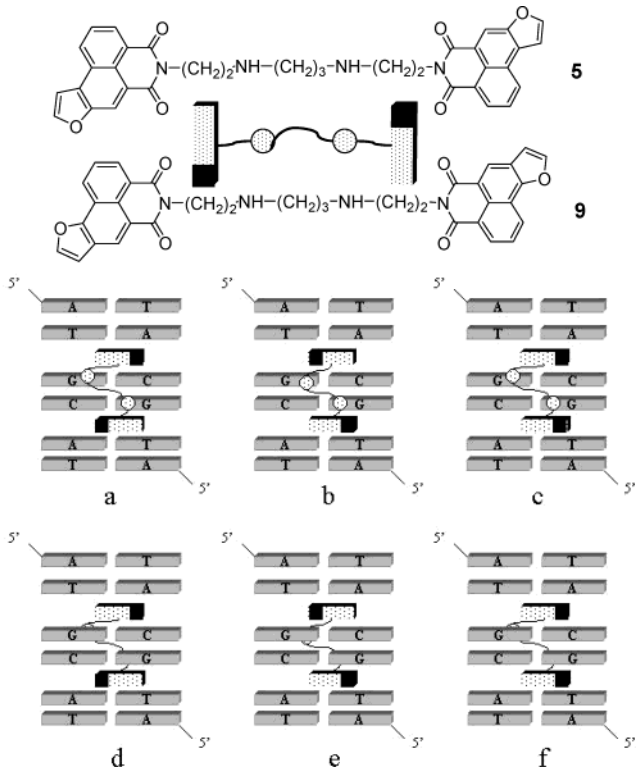

Figure 3. Schematic view of the complexes between compounds **5** and **9** and d(ATGCAT)$_2$. The back square in the chromophores represent the orientation of the furan rings, and the spheres account for the protonated amino groups in the linking chains. Top: complexes with compounds bound through the major groove. (**a**) Relative antiparallel orientation of the chromophores and the furan rings stacked between AC. (**b**) Relative antiparallel orientation of the chromophores and the furan rings stacked between TG. (**c**) Relative parallel orientation of the chromophores. Bottom: complexes in the same relative orientations and with the ligand bound through the minor groove of the DNA hexamer (**d**−**f**).

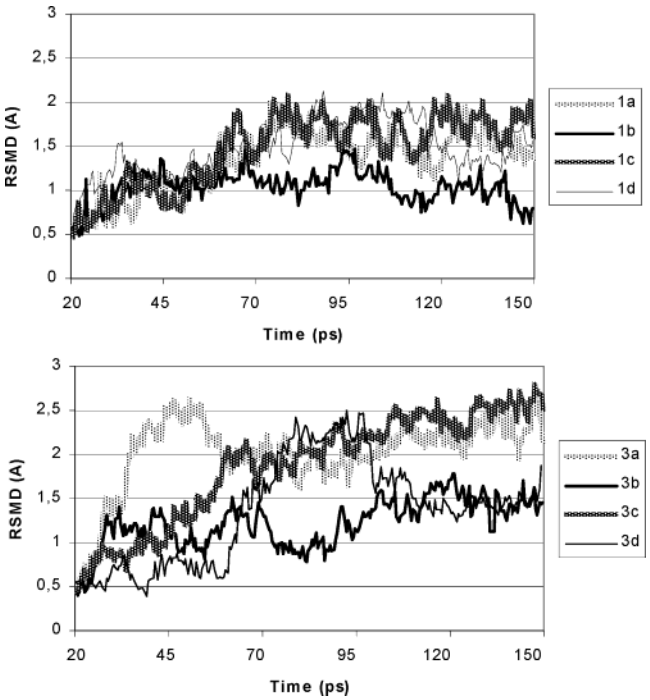

Figure 4. Time evolution (ps) of the root-mean-square deviation (Å) between the simulated structures and the corresponding initial structures (all solute non-hydrogen atoms were included in the comparisons) for complex **1**:(TG)$_2$ (top) and complex **3**:(TG)$_2$ (bottom): (a) side chain in the major groove and the furan ring stacked between TG, (b) side chain in the major groove and the furan ring stacked between AC, (c) side chain in the minor groove and the furan ring stacked between TG, and (d) side chain in the minor groove and the furan ring stacked between AC.

nitrogens of the linking chains and N7 and O6 of the guanines were also monitored along the sampling time. These measurements indicate the presence of either one or two stable hydrogen bonds for all complexes. Figure 6 shows energy-minimized average structures of the last 50 ps of the molecular dynamics simulation for the four complexes. Ligand−DNA interaction energies were also evaluated giving values within the same range for all four complexes. According to these results, no relevant differences can be found in the binding affinity of compounds **5** and **9** to the DNA hexamer through the major groove. In contrast to what happened with related imidazobisnaphthalimides,[3] the length and nature of the linking chain seems to be the appropriate for the process of bisintercalation and the introduction of a furan ring instead of an imidazole one leads to more stable complexes, probably due to better stacking interactions. Although the chromophores are slightly twisted with respect to the orientation adopted by elinafide in its complex with the same DNA hexamer, none of the simulations reported in this work show drastic conformational changes, leading us to propose that the

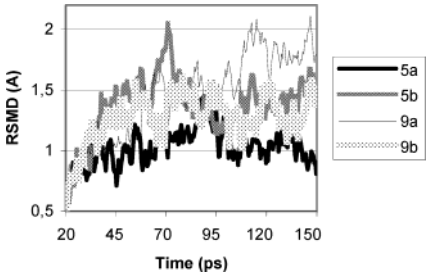

Figure 5. Time evolution (ps) of the root-mean-square deviation (Å) between the simulated structures and the corresponding initial structures (all solute non-hydrogen atoms were included in the comparisons) for complex **5**:d(ATGCAT)$_2$ (a) with the side chain in the major groove and the furan ring stacked between TG, (b) with the side chain in the major groove and the furan ring stacked between AC, and complex **9**:d(ATGCAT)$_2$ (a) with the side chain in the major groove and the furan ring stacked between TG, (b) with the side chain in the major groove and the furan ring stacked between AC.

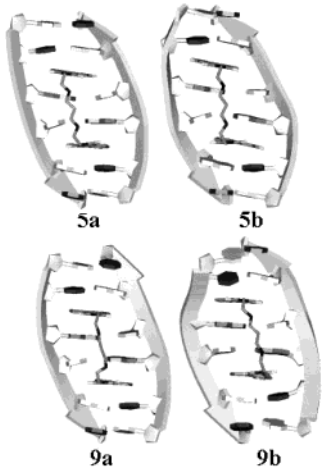

Figure 6. Side views of the energy minimized average structures of the last 50 ps of the molecular dynamics simulations in water for complexes **5a**, **5b**, **9a**, and **9b**.

introduction of the furan ring angularly fused to the naphthalimide moiety, probably leads to better stacking interactions. This possibility was recently pointed out by Bailly and co-workers.[6] However, the possibility of the presence of hydrogen bonds between the furan oxygen and the amino group of the guanine in the minor groove which was postulated in the same work as the principal determinant of GC selectivity shown for compound **5** if compared to elinafide was explored for all the complexes and discarded in all cases.

With respect to the relative orientation of the furan ring with respect to the naphthlimide moiety, that seems to affect the biological activity our simulations do not allow us, so far, to establish any significant difference in the binding affinity. Further computer simulations and analysis of the results will be undertaken in future works.

Mechanism of Action Studies. Compounds **1** and **5** have been extensively studied by Bailly et al.[6] Qualitative binding studies by absorption and melting temperature measurements, as well as quantitative studies using surface plasmon resonance, have established that the dimer binds considerably more tightly to DNA than the corresponding monomer.[6]

In this work compounds **1** and **3** as models of monointercalators and **5** and **9** as models of bisinter-

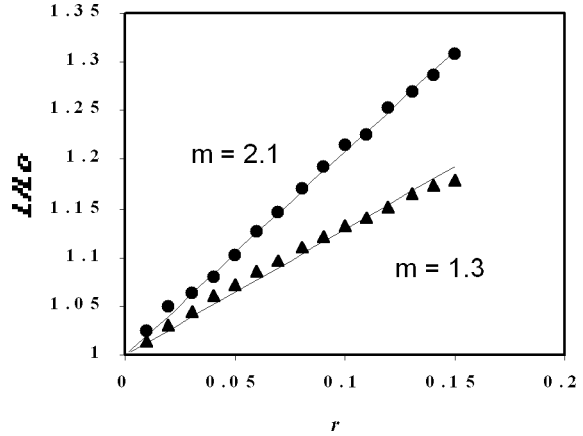

Figure 7. Relative length increase L/L_0 of **1** (▲) and **5** (●) DNA complexes as a function of the molar ratio of added compound to DNA nucleotides (r). The contour lengths in the presence (L) or absence (L_o) of the compounds were calculated from viscosity measurements on sonicated calf thymus DNA.

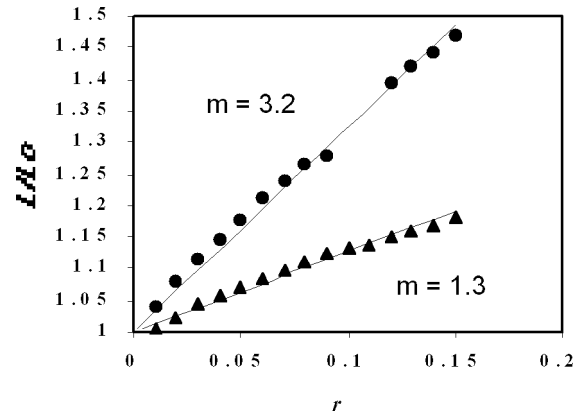

Figure 8. Relative length increase L/L_0 of **3** (▲) and **9** (●) DNA complexes as a function of the molar ratio of added compound to DNA nucleotides (r). The contour lengths in the presence (L) or absence (L_o) of the compounds were calculated from viscosity measurements on sonicated calf thymus DNA.

calators have been studied by viscosimetric titration with calf thymus DNA. It is known that DNA length increases when a drug behaves as an intercalator.[20] When the relative increase in contour length, L/L_0, versus r is plotted, the slope m of this plot has different values depending on the functionality of the intercalator. Monofunctional intercalators such as ethidium bromide, proflavine, and aminoacridines usually have values of m between 0.8 and 1.5.[21] In our case, when L/L_0 is plotted versus r for compounds **1** and **3** (Figures 7 and 8), the least-squares fitting gives a slope of 1.3 for both compounds, indicating that these compounds provoke DNA helix extension as monofunctional intercalators. In the case of compounds **5** and **9**, slopes of 2.1 and 3.2 have been obtained, respectively (Figures 7 and 8), showing that **5** and **9** provoke DNA extension as bifunctional intercalators. For bisintercalators, the slope is expected to be twice the value observed for monointercalators, as it has been verified for a variety of intercalating compounds.[22]

To further evaluate the mechanism of action, compound **9** was selected to carry out the assay of single-cell gel electrophoresis (comet assay). The comet assay detects DNA damage in individual cells embedded in agarose. It is based on the property of negatively

Figure 9. Single cell gel electrophoresis assay for a negative control (PBS) (left), for compound **9** (middle) and for a positive control (doxorubicin) (right).

charged DNA fragments to migrate when an electric field is applied to the gel after cell lysis.[23] Doxorubicin was chosen as a positive reference, and PBS (phosphate-buffered saline, pH = 7.4) was used as a negative control. One hour after the treatment, the samples were observed using a fluorescence microscope, and the DNA damage of compound **9** was similar to the damage of the positive reference (Figure 9). This result suggests that the antitumor activity of this type of mononaphthalimides may be related to their ability to induce DNA damage.

Conclusions

In conclusion, the introduction of a π-excedent furan or thiophene ring fused to the naphthalimide moiety has led to chromophore modified naphthalimides suitable for dimerization. Recently we reported the poor antitumor activities obtained in the dimerization of structurally related imidazonaphthalimides. In that case, molecular modeling techniques put forward the low stability of the corresponding DNA−drug complexes. The present molecular dynamics simulations show that the synthesized bisfuronaphthalimides are capable of forming stable DNA complexes, which is in accordance with their improved in vitro activities, further supported by in vivo experiments. These results, together with the encouraging activities found for the related electron poor pyrazinonaphthalimides, have prompted us to propose that the electronic nature of the heterocycle fused to the naphthalimide moiety does not affect the binding affinity. Most probably, the van der Waals contribution to the staking interactions might be governing the DNA binding process for this type of compounds. At this point, further experimental and theoretical work becomes necessary in order to support this statement.

Experimental Section

General Methods. Melting points (uncorrected) were determined on a Stuart Scientific SMP3 apparatus. Infrared (IR) spectra were recorded with a Perkin-Elmer 1330 infrared spectrophotometer. ^{1}H and ^{13}C NMR: δ values were recorded on a Bruker 300-AC instrument. Chemical shifts (δ) are expressed in parts per million relative to internal tetramethylsilane; coupling constants (J) are in hertz. Mass spectra were run on a HP 5989A spectrometer. Elemental analyses (C, H, N) were performed on a Perkin-Elmer 2400 CHN apparatus at the Microanalyses Service of the University Complutense of Madrid; unless otherwise stated all reported values are within ±0.4% of the theoretical compositions. Thin-layer chromatography (TLC) was run on Merck silica gel 60 F-254 plates. Unless stated otherwise, starting materials used were high-grade commercial products. The photolyses were carried out in a quartz immersion well apparatus with a Pyrex filter and a 400-W medium-pressure Hg arc lamp. Solutions of the compound were purged for 1 h with argon and irradiated under a positive pressure of argon.

2-[(1-Methoxycarbonyl)-2-(3-thienyl)vinyl]benzoic Acid (16). To a solution of dimethyl homophthalate[24] (1.0 g, 4.80 mmol) in dry THF (9 mL) at 0 °C under argon was added 3-thiophenecarbaldehyde (0.54 g, 4.80 mL). Then, sodium hydride (0.16 g, 5.00 mmol of a 80% oil dispersion) was added in portions. When the addition was complete, the reaction was allowed to warm to room temperature and was stirred for 24 h. The reaction crude was diluted with diethyl ether (14 mL) and filtered. The residue was dissolved in water (16 mL) and the pH adjusted to 5 with 1 N aqueous oxalic acid. The precipitate formed was collected by filtration to give **16** (1.29 g, 93%) as a white solid, mp 148−150 °C (AcOEt/hexane). IR (KBr): 3100, 1720, 1675 cm^{-1}. ^{1}H NMR ($CDCl_3$): δ 8.21 (dd, 1H, J = 7.7 and 1.1 Hz, ArH), 7.81 (s, 1H, CH=C), 7.54 (m, 2H, ArH), 7.25 (d, 1H, J = 7.7 Hz, ArH), 7.02 (m, 2H, ArH), 6.34 (dd, 1H, J = 4.9 and 1.1 Hz, ArH), 3.70 (s, 3H, CH_3). ^{13}C NMR ($CDCl_3$): δ 171.4, 168.0, 138.6, 136.5, 133.4, 132.2, 131.7, 131.6, 130.9, 129.2, 129.0, 128.3, 127.9, 125.5, 52.2. Anal. ($C_{15}H_{12}O_4S$) C, H, S.

Naphtho[1,2-*b*]thiophene-5,6-dicarboxylic Anhydride (20). A mixture of **16** (300 mg, 1.05 mmol) and iodine (275 mg, 1.10 mmol) in absolute EtOH (400 mL) was photolyzed for 8 h. Then, a solution of aqueous NaOH (2.2 mL, 1 M) was added, followed by saturated $NaHSO_3$ (1.1 mL). The solvent was removed under reduced pressure and the residue suspended in water (3.8 mL). After standing overnight, the precipitate was collected by filtration and washed with water. The solid was suspended in acetic anhydride (2.0 mL) and heated on a steam bath for 15 min. Then, the solution was allowed to stand at room-temperature overnight. The product was isolated by filtration and washed with AcOEt to give **20** (146 mg, 55%) as a yellow solid, mp >300 °C ($CHCl_3$). IR (KBr): 1770, 1730 cm^{-1}. ^{1}H NMR (DMSO-d_6/CF_3CO_2D): δ 9.63 (s, 1H, ArH), 9.33 (d, 1H, J = 8.5 Hz, ArH), 9.11 (d, 1H, J = 7.3 Hz, ArH), 8.73 (d, 1H, J = 5.0 Hz, thiopheneH), 8.57 (m, 1H, ArH), 8.51 (d, 1H, J = 5.0 Hz, thiopheneH). ^{13}C NMR ($CDCl_3$): δ 161.0, 160.8, 152.1, 138.0, 131.8, 130.7, 130.5, 129.3, 128.1, 127.9, 127.8, 126.2, 118.7, 107.6. Anal. ($C_{14}H_6O_3S$) C, H, S.

Naphtho[2,1-*b*]thiophene-5,6-dicarboxylic Anhydride (18). The procedure described above was used for the synthesis of **18**. From **14**[25] (300 mg, 1.05 mmol) and iodine (275 mg, 1.10 mmol) in absolute EtOH (400 mL), **18** (30 mg, 11%) was obtained as a yellow solid, mp >300 °C ($CHCl_3$). IR (KBr): 1770, 1730 cm^{-1}. ^{1}H NMR ($CDCl_3$): δ 9.11 (s, 1H, ArH), 8.76 (d, 1H, J = 8.2 Hz, ArH), 8.66 (d, 1H, J = 7.2 Hz, ArH), 8.15 (d, 1H, J = 5.5 Hz, thiopheneH), 8.08 (d, 1H, J = 5.5 Hz, thiopheneH), 7.93 (m, 1H, ArH). ^{13}C NMR ($CDCl_3$): δ 161.0, 160.9, 151.0, 144.7, 134.1, 131.6, 131.0, 130.9, 129.6, 129.0, 127.7, 122.3, 121.7, 112.6. Anal. ($C_{14}H_6O_3S$) C, H, S.

General Procedure for the Preparation of Mononaphthalimides 1−4 and Their Salts. A suspension of the adequate anhydride (1 equiv) in toluene was treated with N^1,N^1-dimethyl-1,2-ethanediamine (1 equiv) in absolute EtOH. The mixture was heated at reflux temperature until the reaction was completed (TLC). The precipitated solid was filtered and recrystallized from the appropriate solvent to

provide the mononaphthalimide as a free base. This compound was converted into the corresponding hydrochloride (**1** and **3**) or methanosulfonate (**2** and **4**). For the synthesis of hydrochlorides, a suspension of the free base in absolute EtOH was saturated with HCl (g) for 2 h, and the solid formed was filtered. For the synthesis of methanesulfonates, the free base was suspended in absolute EtOH and methanesulfonic acid (2.2 equiv) was added. The monoimide salt was isolated by filtration and washed with diethyl ether.

5-[2-(Dimethylamino)ethyl]benz[*de*]thieno[3,2-*g*]isoquinoline-4,6(5*H*)-dione (2). From **18** (100 mg, 0.39 mmol) in toluene (2.5 mL) and N^1,N^1-dimethyl-1,2-ethanediamine (34 mg, 0.39 mmol) in absolute EtOH (1 mL) yielded **2** (103 mg, 81%) as a yellow solid, mp 181−182 °C (absolute EtOH/toluene). IR (KBr): 1690, 1660 cm^{-1}. ^1H NMR (DMSO-d_6): δ 9.24 (s, 1H, ArH), 9.10 (d, 1H, J = 8.5 Hz, ArH), 8.60 (d, 1H, J = 6.7 Hz, ArH), 8.55 (d, 1H, J = 5.5 Hz, thiopheneH), 8.48 (d, 1H, J = 5.5 Hz, thiopheneH), 8.06 (m, 1H, ArH), 4.28 (t, 2H, J = 7.3 Hz, CH_2), 2.62 (t, 2H, J = 7.3 Hz, CH_2), 2.31 (s, 6H, $2CH_3$). The free base was converted into the corresponding methanesulfonate trihydrate (70%), mp 197−199 °C. IR (KBr): 2650, 1690, 1650 cm^{-1}. ^1H NMR (DMSO-d_6): δ 9.23 (s, 1H, ArH), 9.09 (d, 1H, J = 7.9 Hz, ArH), 8.59 (d, 1H, J = 7.3 Hz, ArH), 8.54 (d, 1H, J = 4.9 Hz, thiopheneH), 8.47 (d, 1H, J = 4.9 Hz, thiopheneH), 8.05 (dd, 1H, J = 7.9 and 7.3 Hz, ArH), 4.49 (br s, 2H, CH_2), 3.55 (br s, 2H, CH_2), 3.00 (s, 6H, $2CH_3N$), 2.36 (s, 3H, $CH_3SO_3^-$). ^{13}C NMR (DMSO-d_6): δ 164.3, 164.1, 140.1, 137.2, 134.8, 130.7, 129.2, 127.5, 127.3, 127.1, 125.4, 123.2, 122.6, 118.3, 55.0, 42.9, 39.7, 35.3. Anal. ($C_{18}H_{16}N_2O_2S\cdot CH_3SO_3H\cdot 3H_2O$) C, H, N, S.

5-[2-(Dimethylamino)ethyl]benz[*de*]furo[2,3-*g*]isoquinoline-4,6(5*H*)-dione (3). From **19**[5] (200 mg, 0.84 mmol) in toluene (5 mL) and N^1,N^1-dimethyl-1,2-ethanediamine (74 mg, 0.84 mmol) in absolute EtOH (2 mL) yielded **3** (160 mg, 62%) as a yellow solid, mp 178−180 °C (absolute EtOH/toluene). IR (KBr): 1690, 1650 cm^{-1}. ^1H NMR (DMSO-d_6): δ 8.84 (s, 1H, ArH), 8.69 (d, 1H, J = 8.6 Hz, ArH), 8.51 (d, 1H, J = 7.3 Hz, ArH), 8.39 (d, 1H, J = 2.4 Hz, furanH), 7.98 (m, 1H, ArH), 7.39 (d, 1H, J = 2.4 Hz, furanH), 4.18 (t, 2H, J = 6.7 Hz, CH_2), 2.51 (m, 2H, CH_2), 2.21 (s, 6H, $2CH_3$). The free base (140 mg, 0.46 mmol) was converted into the corresponding hydrochloride 2.5hydrate (116 mg, 74%), mp >300 °C. IR (KBr): 3400, 2810, 2760, 1690, 1655 cm^{-1}. ^1H NMR (DMSO-d_6): δ 9.73 (br s, 1H, NH^+), 8.90 (s, 1H, ArH), 8.76 (d, 1H, J = 8.5 Hz, ArH), 8.56 (d, 1H, J = 7.3 Hz, ArH), 8.42 (d, 1H, J = 2.5 Hz, furanH), 8.02 (m, 1H, ArH), 7.43 (d, 1H, J = 2.5 Hz, furanH), 4.43 (dd, 2H, J = 6.1 and 5.5 Hz, CH_2), 3.47 (br s, 2H, CH_2), 2.90 (s, 6H, $2CH_3$). ^{13}C NMR (D_2O): δ 165.4, 165.0, 153.4, 148.0, 130.6, 127.9, 127.7, 124.8, 124.7, 120.5, 118.2, 115.7, 109.1, 55.8, 44.3, 36.1. MS (ESI): m/z 309 $[M + H]^+$. Anal. ($C_{18}H_{16}N_2O_3\cdot HCl\cdot 2.5H_2O$) C, H, N.

5-[2-(Dimethylamino)ethyl]benz[*de*]thieno[2,3-*g*]isoquinoline-4,6(5*H*)-dione (4). From **20** (200 mg, 0.79 mmol) in toluene (5 mL) and N^1,N^1-dimethyl-1,2-ethanediamine (70 mg, 0.79 mmol) in absolute EtOH (2 mL) yielded **4** (204 mg, 80%) as a yellow solid, mp 179−181 °C (toluene). IR (KBr): 1695, 1655 cm^{-1}. ^1H NMR (DMSO-d_6/CF_3CO_2D): δ 8.92 (s, 1H, ArH), 8.60 (d, 1H, J = 7.9 Hz, ArH), 8.49 (d, 1H, J = 7.3 Hz, ArH), 8.09 (d, 1H, J = 5.5 Hz, thiopheneH), 7.94 (m, 1H, ArH), 7.89 (d, 1H, J = 5.5 Hz, thiopheneH), 4.44 (t, 2H, J = 5.5 Hz, CH_2), 3.52 (t, 2H, J = 5.5 Hz, CH_2), 2.96 (s, 6H, $2CH_3$). The free base was converted into the corresponding methanesulfonate dihydrate (82%), mp 217−220 °C. IR (KBr): 2620, 2450, 1700, 1650 cm^{-1}. ^1H NMR (DMSO-d_6): δ 9.24 (br s, 1H, NH^+), 9.00 (s, 1H, ArH), 8.70 (d, 1H, J = 7.9 Hz, ArH), 8.55 (d, 1H, J = 6.7 Hz, ArH), 8.18 (d, 1H, J = 4.3 Hz, thiopheneH), 8.00 (m, 2H, thiopheneH, ArH), 4.48 (br s, 2H, CH_2), 3.50 (br s, 2H, CH_2), 3.00 (s, 6H, $2NCH_3$), 2.35 (s, 3H, $CH_3SO_3^-$). ^{13}C NMR (DMSO-d_6): δ 164.0, 163.9, 142.2, 137.4, 129.6, 129.3, 129.0, 127.9, 127.7, 126.6, 124.6, 122.9, 119.3, 54.9, 42.8, 39.6, 35.3. Anal. ($C_{18}H_{16}N_2O_2S\cdot CH_3SO_3H\cdot 2H_2O$) C, H, N, S.

General Procedure for the Preparation of Bisnaphthalimides 5−12 and Their Salts. A suspension of the adequate anhydride (2 equiv) in toluene was treated with the corresponding polyamine (1 equiv) in ethanol. The mixture was heated at reflux temperature until the reaction was completed (TLC). The precipitated solid was filtered and recrystallized from the appropriate solvent to provide the bisnaphthalimide as a free base. This compound was suspended in absolute EtOH and methanesulfonic acid (2.5 equiv) was added. The bisimide salt was isolated by filtration and washed with diethyl ether.

***N*,*N*′-Bis[2-(4,6-dioxo-5,6-dihydro-4*H*-benz[*de*]furo[3,2-*g*]isoquinolin-5-yl)ethyl]-*N*,*N*′-dimethyl-1,3-propanediamine (6).** To a suspension of compound **17**[5] (168 mg, 0.70 mmol) in DMF (3 mL), was added dropwise *N*,*N*′-bis(2-aminoethyl)-*N*,*N*′-dimethyl-1,3-propanediamine (60 mg, 0.32 mmol) in DMF (2 mL). The mixture was heated at 80 °C for 7 h and then was allowed to stand at room-temperature overnight. The precipitated solid was isolated by filtration to give **6** (92 mg, 46%) as a yellow solid, mp 167−170 °C (DMF). IR (KBr): 1695, 1655 cm^{-1}. ^1H NMR (DMSO-d_6/CF_3CO_2D): δ 9.68 (br s, 2H, $2NH^+$), 8.83 (d, 2H, J = 7.9 Hz, ArH), 8.72 (s, 2H, ArH), 8.52 (m, 4H, furanH, ArH), 7.96 (dd, 2H, J = 7.9 and 7.3 Hz, ArH), 7.87 (m, 2H, furanH), 4.46 (br s, 4H, $2CH_2N$), 3.44 (br s, 4H, $2CH_2N$), 3.28 (br s, 4H, $2CH_2N$), 3.00 (s, 6H, $2CH_3$), 2.13 (br s, 2H, CH_2). ^{13}C NMR (DMSO-d_6/CF_3CO_2D): δ 164.3, 164.2, 151.6, 150.7, 130.8, 129.4, 127.5, 125.9, 125.0, 122.8, 118.8, 117.1, 116.9, 107.2, 53.0, 52.2, 52.1, 35.1, 30.8. MS (ESI): m/z 629 $[M + H]^+$. Anal. ($C_{37}H_{32}N_4O_6$) C, H, N.

***N*,*N*′-Bis[2-(4,6-dioxo-5,6-dihydro-4*H*-benz[*de*]thieno[3,2-*g*]isoquinolin-5-yl)ethyl]-1,3-propanediamine (7).** Following the general procedure, from **18** (100 mg, 0.39 mmol) in toluene (2.5 mL) and *N*,*N*′-bis(2-aminoethyl)-1,3-propanediamine (32 mg, 0.20 mmol) in absolute EtOH (1 mL) was obtained **7** (83 mg, 67%) as a yellow solid, mp 204 °C (dec) (absolute EtOH/toluene). IR (KBr): 3400, 3090, 1690, 1650 cm^{-1}. ^1H NMR (DMSO-d_6/CF_3CO_2D): δ 9.15 (s, 2H, ArH), 9.02 (d, 2H, J = 7.9 Hz, ArH), 8.90 (br s, 4H, $2NH_2^+$), 8.51 (d, 2H, J = 7.9 Hz, ArH), 8.45 (d, 2H, J = 4.9 Hz, thiopheneH), 8.40 (d, 2H, J = 4.9 Hz, thiopheneH), 7.97 (t, 2H, J = 7.9 Hz, ArH), 4.39 (br s, 4H, $2CH_2N$), 3.34 (br s, 4H, $2CH_2N$), 3.06 (br s, 4H, $2CH_2N$), 1.93 (br s, 2H, CH_2). The free base was converted into the corresponding dimethanesulfonate trihydrate (96%), mp 188 °C (dec). IR (KBr): 3400, 2800, 1690, 1650 cm^{-1}. ^1H NMR (DMSO-d_6): δ 9.18 (s, 2H, ArH), 9.05 (d, 2H, J = 7.9 Hz, ArH), 8.64 (br s, 4H, $2NH_2^+$), 8.53 (d, 2H, J = 7.9 Hz, ArH), 8.49 (d, 2H, J = 4.9 Hz, thiopheneH), 8.41 (d, 2H, J = 4.9 Hz, thiopheneH), 7.99 (t, 2H, J = 7.9 Hz, ArH), 4.40 (br s, 4H, $2CH_2N$), 3.34 (br s, 4H, $2CH_2N$), 3.07 (br s, 4H, $2CH_2N$), 2.31 (s, 6H, $2CH_3$), 1.94 (br s, 2H, CH_2). ^{13}C NMR (DMSO-d_6): δ 164.3, 164.1, 140.1, 137.2, 134.8, 130.7, 130.5, 129.2, 127.5, 127.1, 125.4, 123.2, 122.6, 118.4, 45.4, 44.3, 39.7, 36.6, 22.1. Anal. ($C_{35}H_{28}N_4O_4S_2\cdot 2CH_3SO_3H\cdot 3H_2O$) C, H, N, S.

***N*,*N*′-Bis[2-(4,6-dioxo-5,6-dihydro-4*H*-benz[*de*]thieno[3,2-*g*]isoquinolin-5-yl)ethyl]-*N*,*N*′-dimethyl-1,3-propanediamine (8).** To a hot suspension of compound **18** (67 mg, 0.26 mmol) in DMF (2.5 mL) was added dropwise *N*,*N*′-bis(2-aminoethyl)-*N*,*N*′-dimethyl-1,3-propanediamine (25 mg, 0.13 mmol) in DMF (1 mL). After the mixture was refluxed for 2 h, an excess of *N*,*N*′-bis(2-aminoethyl)-*N*,*N*′-dimethyl-1,3-propanediamine (12 mg, 0.06 mmol) was added. The reaction mixture was refluxed for an additional 3 h, and then the solution was allowed to stand at room-temperature overnight. The precipitate was isolated by filtration to give **8** (49 mg, 57%) as a yellow solid, mp 172−174 °C (DMF). IR (KBr): 1700, 1660 cm^{-1}. ^1H NMR (DMSO-d_6/CF_3CO_2D): δ 9.18 (s, 2H, ArH), 9.02 (d, 2H, J = 7.9 Hz, ArH), 8.56 (d, 2H, J = 7.3 Hz, ArH), 8.46 (d, 2H, J = 5.5 Hz, thiopheneH), 8.40 (d, 2H, J = 5.5 Hz, thiopheneH), 7.98 (dd, 2H, J = 7.9 and 7.3 Hz, ArH), 4.54 (br s, 4H, $2CH_2N$), 3.62 (br s, 4H, $2CH_2N$), 3.51 (br s, 2H, CH_2N), 3.34 (br s, 2H, CH_2N), 3.05 (s, 6H, $2CH_3$), 2.18 (br s, 2H, CH_2). The free base was converted into the corresponding dimethanesulfonate dihydrate (63%), mp 154 °C (dec). IR (KBr): 2620, 1690, 1650 cm^{-1}. ^1H NMR (DMSO-d_6): δ 9.47 (br s, 2H, $2NH^+$), 9.15 (s, 2H, ArH), 9.00 (d, 2H, J = 7.9 Hz, ArH), 8.51 (d, 2H, J = 7.3 Hz, ArH), 8.44 (d, 2H, J = 5.5 Hz, thiopheneH), 8.39 (d, 2H, J = 5.5 Hz, thiopheneH), 7.95 (m, 2H, ArH), 4.47 (br

s, 4H, $2CH_2N$), 3.45 (br s, 4H, $2CH_2N$), 3.28 (br s, 4H, $2CH_2N$), 2.99 (s, 6H, $2CH_3N$), 2.29 (s, 6H, $2CH_3SO_3^-$), 2.14 (br s, 2H, CH_2). ^{13}C NMR (DMSO-d_6): δ 164.2, 164.0, 140.1, 137.1, 134.8, 130.7, 129.2, 127.4, 127.3, 127.1, 125.3, 123.1, 122.4, 118.2, 56.0, 52.8, 52.1, 40.1, 39.7, 34.8. Anal. ($C_{37}H_{32}N_4O_4S_2 \cdot 2CH_3SO_3H \cdot 2H_2O$) C, H, N, S.

***N,N′*-Bis[2-(4,6-dioxo-5,6-dihydro-4*H*-benz[*de*]furo[2,3-*g*]isoquinolin-5-yl)ethyl]-1,3-propanediamine (9).** Following the general procedure, from **19**[5] (150 mg, 0.63 mmol) in toluene (7 mL) and *N,N′*-bis(2-aminoethyl)-1,3-propanediamine (51 mg, 0.32 mmol) in absolute EtOH (2 mL) was obtained **9** (138 mg, 72%) as a yellow solid, mp 126−129 °C (absolute EtOH/toluene). IR (KBr): 3480, 1690, 1645 cm^{-1}. ^{1}H NMR (CF_3CO_2D): δ 9.00 (s, 2H, ArH), 8.90 (d, 2H, J = 7.4 Hz, ArH), 8.71 (d, 2H, J = 6.0 Hz, ArH), 8.01 (m, 4H, furanH, ArH), 7.19 (d, 2H, J = 2.0 Hz, furanH), 4.84 (m, 4H, $2CH_2N$), 3.88 (m, 4H, $2CH_2N$), 3.59 (m, 4H, $2CH_2N$), 2.56 (m, 2H, CH_2). The free base was converted into the corresponding dimethanesulfonate trihydrate (56%), mp 217−220 °C. IR (KBr): 3400, 2750, 1690, 1645 cm^{-1}. ^{1}H NMR (D_2O): δ 7.41 (s, 2H, ArH), 7.31 (d, 2H, J = 7.3 Hz, ArH), 7.25 (m, 4H, furanH, ArH), 6.84 (dd, 2H, J = 8.3 and 7.3 Hz, ArH), 6.37 (m, 2H, furanH), 3.80 (m, 4H, $2CH_2N$), 3.05 (m, 8H, $4CH_2N$), 2.53 (s, 6H, $2CH_3$), 1.97 (m, 2H, CH_2). ^{13}C NMR (D_2O): δ 165.2, 164.8, 152.9, 147.8, 130.1, 127.6, 127.3, 127.1, 124.3, 124.0, 119.9, 117.5, 115.1, 108.7, 45.8, 44.7, 39.4, 37.0, 21.6. Anal. ($C_{35}H_{28}N_4O_6 \cdot 2CH_3SO_3H \cdot 3H_2O$) C, H, N, S.

***N,N′*-Bis[2-(4,6-dioxo-5,6-dihydro-4*H*-benz[*de*]furo[2,3-*g*]isoquinolin-5-yl)ethyl]-*N,N′*-dimethyl-1,3-propanediamine (10).** Following the general procedure, from **19**[5] (190 mg, 0.80 mmol) in toluene (5 mL) and *N,N′*-bis(2-aminoethyl)-*N,N′*-dimethyl-1,3-propanediamine (75 mg, 0.40 mmol) in absolute EtOH (2 mL) was obtained **10** (68 mg, 27%) as an unstable brown solid. The free base was converted into the corresponding dimethanesulfonate dihydrate (75%), mp 255−257 °C. IR (KBr): 2650, 1695, 1650 cm^{-1}.^{1}H NMR (DMSO-d_6): δ 9.45 (br s, 2H, $2NH^+$), 8.83 (s, 2H, ArH), 8.68 (d, 2H, J = 7.9 Hz, ArH), 8.51 (d, 2H, J = 7.3 Hz, ArH), 8.38 (m, 2H, furanH), 7.97 (m, 2H, ArH), 7.36 (m, 2H, furanH), 3.43 (m, 4H, $2CH_2N$), 3.42 (m, 4H, $2CH_2N$), 3.40 (br s, 4H, $2CH_2N$), 2.95 (s, 6H, $2CH_3N$), 2.28 (s, 6H, $2CH_3SO_3^-$), 2.09 (m, 2H, CH_2). ^{13}C NMR (DMSO-d_6): δ 164.0, 163.7, 152.6, 147.8, 129.4, 127.7, 126.9, 126.3, 125.5, 124.1, 122.5, 118.5, 117.8, 108.8, 72.3, 60.2, 52.8, 52.4, 39.6, 35.1. MS (ESI): m/z 629 [M + H]$^+$. Anal. ($C_{37}H_{32}N_4O_6 \cdot 2CH_3SO_3H \cdot 2H_2O$) C, H, N, S.

***N,N′*-Bis[2-(4,6-dioxo-5,6-dihydro-4*H*-benz[*de*]thieno-[2,3-*g*]isoquinolin-5-yl)ethyl]-1,3-propanediamine (11).** To a suspension of compound **20** (200 mg, 0.79 mmol) in toluene (5 mL) was added dropwise *N,N′*-bis(2-aminoethyl)-1,3-propanediamine (63 mg, 0.39 mmol) in absolute EtOH (2 mL). After the mixture was refluxed for 4 h, an excess of *N,N′*-bis(2-aminoethyl)-1,3-propanediamine (10 mg, 0.06 mmol) was added. The reaction mixture was refluxed for 2 additional hours, and then the precipitate was isolated by filtration to give **11** (207 mg, 84%) as a yellow solid, mp 168−170 °C (absolute EtOH/toluene). IR (KBr): 3325, 1690, 1650 cm^{-1}. ^{1}H NMR (DMSO-d_6/ CF_3CO_2D): δ 8.94 (s, 2H, ArH), 8.84 (br s, 4H, $2NH_2^+$), 8.64 (d, 2H, J = 7.9 Hz, ArH), 8.49 (d, 2H, J = 7.3 Hz, ArH), 8.11 (d, 2H, J = 4.9 Hz, thiopheneH), 7.93 (m, 4H, thiopheneH, ArH), 4.39 (br s, 4H, $2CH_2N$), 3.35 (br s, 4H, $2CH_2N$), 3.07 (br s, 4H, $2CH_2N$), 1.93 (br s, 2H, CH_2). The free base was converted into the corresponding dimethanesulfonate monohydrate (92%), mp 212 °C (dec). IR (KBr): 3400, 2800, 1700, 1650 cm^{-1}. ^{1}H NMR (DMSO-d_6): δ 8.93 (s, 2H, ArH), 8.64 (d, 6H, J = 7.9 Hz, ArH, $2NH_2^+$), 8.48 (d, 2H, J = 7.3 Hz, ArH), 8.11 (d, 2H, J = 4.9 Hz, thiopheneH), 7.94 (dd, 2H, J = 7.9 and 7.3 Hz, ArH), 7.91 (d, 2H, J = 4.9 Hz, thiopheneH), 4.38 (br s, 4H, $2CH_2N$), 3.38 (br s, 4H, $2CH_2N$), 3.07 (br s, 4H, $2CH_2N$), 2.27 (s, 6H, $2CH_3$), 1.94 (br s, 2H, CH_2). ^{13}C NMR (DMSO-d_6): δ 165.2, 165.1, 143.3, 138.0, 130.5, 130.4, 129.8, 128.7, 128.6, 128.5, 127.3, 125.1, 123.1, 119.5, 46.5, 44.9, 40.1, 37.4, 22.8. Anal. ($C_{35}H_{28}N_4O_4S_2 \cdot 2CH_3SO_3H \cdot H_2O$) C, H, N, S.

***N,N′*-Bis[2-(4,6-dioxo-5,6-dihydro-4*H*-benz[*de*]thieno-[2,3-*g*]isoquinolin-5-yl)ethyl]-*N,N′*-dimethyl-1,3-propanediamine (12).** To a suspension of compound **20** (200 mg, 0.79 mmol) in toluene (5 mL) was added dropwise *N,N′*-bis(2-aminoethyl)-*N,N′*-dimethyl-1,3-propanediamine (74 mg, 0.39 mmol) in absolute EtOH (2 mL). After the mixture was refluxed for 4 h, an excess of *N,N′*-bis(2-aminoethyl)-*N,N′*-dimethyl-1,3-propanediamine (39 mg, 0.20 mmol) in DMF (4 mL) was added. The reaction mixture was refluxed for 3 days and then was allowed to stand at room-temperature overnight. The precipitate was isolated by filtration to give **12** (71 mg, 28%) as a yellow solid, mp 164−168 °C (DMF). IR (KBr): 1700, 1660 cm^{-1}.^{1}H NMR (DMSO-d_6/CF_3CO_2D): δ 8.95 (s, 2H, ArH), 8.63 (d, 2H, J = 7.9 Hz, ArH), 8.53 (d, 2H, J = 6.7 Hz, ArH), 8.09 (d, 2H, J = 5.0 Hz, thiopheneH), 7.93 (m, 2H, ArH), 7.87 (d, 2H, J = 5.0 Hz, thiopheneH), 4.53 (br s, 4H, $2CH_2N$), 3.60 (br s, 4H, $2CH_2N$), 3.48 (br s, 2H, CH_2N), 3.34 (br s, 2H, CH_2N), 3.05 (s, 6H, $2CH_3$), 2.19 (br s, 2H, CH_2). The free base was converted into the corresponding dimethanesulfonate tetrahydrate (61%), mp 163−168 °C (absolute EtOH/toluene). IR (KBr): 2400, 1700, 1650 cm^{-1}. ^{1}H NMR (DMSO-d_6): δ 9.59 (br s, 2H, $2NH^+$), 9.03 (br s, 2H, ArH), 8.73 (br s, 2H, ArH), 8.59 (br s, 2H, ArH), 8.18 (br s, 2H, ArH), 8.01 (br s, 2H, ArH), 7.96 (br s, 2H, ArH), 4.55 (br s, 4H, $2CH_2N$), 3.56 (br s, 4H, $2CH_2N$), 3.37 (br s, 4H, $2CH_2N$), 3.08 (s, 6H, $2CH_3N$), 2.37 (s, 6H, $2CH_3SO_3^-$), 2.21 (br s, 2H, CH_2). ^{13}C NMR (DMSO-d_6): δ 164.1, 163.9, 142.3, 137.4, 129.8, 129.4, 129.1, 128.0, 127.8, 126.7, 126.6, 124.7, 122.9, 119.3, 52.7, 52.1, 52.0, 40.1, 39.6, 34.8. Anal. ($C_{37}H_{32}N_4O_4S_2 \cdot 2CH_3SO_3H \cdot 4H_2O$) C, H, N, S.

In Vitro Cytotoxicity Assays. The cell lines used were human colon carcinoma (HT-29) (ATCC, HTB 38), human cervical carcinoma (HeLa) (ATCC, CCL 2), and human prostate carcinoma (PC-3) (ECACC, 90112714). For each experiment, cultures were seeded from frozen stocks. Each cell line was maintained in its appropriate medium and was incubated at 37 °C in a 5% CO_2 atmosphere.

All cell lines were in the logarithmic phase of growth when the assay of 3-(4,5-dimethylthiazol-2-yl)-2,5-diphenyltetrazolium bromide (MTT) was carried out. Cells were harvested and seeded into 96-well tissue culture plates at a density of 2.5×10^3 cells/well in 150 μL aliquots of medium. The concentrations tested were serial dilutions of a stock solution (1×10^{-5} M in DMSO) with phosphate-buffered saline (PBS) and were added 24 h later. The assay was ended after 72 h of drug exposure and PBS was used as a negative control and doxorubicin as a positive control.

After a 72 h exposure period, cells were washed twice with PBS, and then 50 μL/well of MTT reagent (1 mg/mL in PBS; Sigma) together with 150 μL/well of prewarmed medium were added. The plates were returned to the incubator for 4 h. Subsequently, DMSO was added as solvent. Absorbance was determined at 570 nm with a Microplate reader (Opsys MR).

All experiments were performed at least three times, and the average of the percentage absorbance was plotted against concentration. Then, the concentration of drug required to inhibit 50% of cell growth (IC_{50}) was calculated for each compound.

In Vivo Antitumoral Evaluation. Human tumor xenografts were established by s.c. injection of HT-29 cell line in athymic *nu/nu* nude mice. Mice were kept under standard laboratory conditions according to the guidelines of the Spanish Government. Cells were trypsinized and resuspended in DMEM just before inoculation (10^6 cells/0.1 mL). When tumors reached a volume of ~0.1 cm^3, mice were randomized to a control and treated group (four mice each). The compound was administered ip, dissolved in sterile 0.9% NaCl. Control mice received an equivalent volume of vehicle alone, following an identical schedule. Tumor size was measured 1−2 times per week, and the volumes were calculated using the equation $V = (Dd^2)/2$, where V (nm^3) is tumoral volume, D is longest diameter in mm, and d is shortest diameter in mm.

DNA Binding Experiments. DNA. Calf thymus DNA was purchased from Sigma Chemical Co. as the highly polymerized sodium salt. For viscometric experiments, the DNA was sonicated to fragments of approximately 4.5×10^5 D determined as described by Eigner and Doty.[26] The sonicated DNA

sample displayed an A_{260}/A_{280} ratio of 1.92. This spectral data is consistent with published values.[27]

Viscometric Titrations. The viscometric measurements were performed in an Ubbelohde microviscometer at 25 ± 0.05 °C. Solutions of sonicated DNA and the selected compound were prepared in Tris buffer (50 mM, pH = 6.9). These solutions had different molar ratio, *r*, of added compound to DNA nucleotides. Flow rates were measured with a Schott-Geräte Viscosystem AVS 350 to an accuracy of 0.01%. Time readings were recorded in triplicate to 0.01s.

Alkaline Single Cell Gel Electrophoresis Assay. The alkaline single cell gel electrophoresis assay (comet assay) detects DNA damage in individual cells embedded in agarose. The test was performed on HT-29 cells following the method described by Moinet-Hedin et al.[23] After 1 h of treatment with the drug, cells were centrifuged and resuspended in low-melting-point (LMP) agarose at 37 °C. The cell suspension was put on a slide precoated with normal agarose, and a glass cover slip was added. After solidification at 0 °C, the glass cover slip was gently removed, and a third layer of 0.5% of LMP agarose in PBS was added and run for solidification.

The slides were put in a lysis solution (2.5 M NaCl, 0.1 M EDTA, 10 mM Tris, pH 10, with freshly added 1% Triton X-100 and 10% DMSO) for 1 h and were rinsed in the electrophoresis buffer (0.3 M NaOH, 1 mM EDTA, pH 13) for 40 min. Electrophoresis (300 mA, 0.7 V/cm) was then performed for 24 min in fresh buffer. The slides were washed twice in neutralization buffer (0.4 M Tris, pH 7.5) and stained with ethidium bromide (20 μg/mL). They were observed using a fluorescence microscope (Nikon) with an excitation filter of 515−560 nm and a barrier filter of 580 nm.

Acknowledgment. We thank Federico Gago for helpful comments and discussion. This work was supported by the Dirección General de Estudios Superiores (Grant No. PB98-0055), CYTED and Universidad San Pablo-CEU (Grant No 5-99/01). M.C. thanks Fundación Ramón Areces for finantial support and M. A. G. acknowledges Fundación Universitaria San Pablo CEU for a predoctoral fellowship. We thank the CIEMAT (Spain) for computer time and facilities.

Supporting Information Available: Computational methods: AMBER parameters and partial atomic charges for compounds **1**, **3**, **5**, and **9** (Tables 2−5). This material is available free of charge via the Internet at http://pubs.acs.org.

References

(1) Malviya, V. K.; Liu, P. Y.; Alberts, D. S.; Surwit, E. A.; Craig, J. B.; Hanningan, E. V. Evaluation of Amonafide in Cervical Cancer, Phase II. A SWOG Study. *Am. J. Clin. Oncol.* **1992**, *15*, 41−44.

(2) Bousquet, P. F.; Braña, M. F.; Conlon, D.; Fitzgerald, K. M.; Perron, D.; Cocchiaro, C.; Miller, R.; Moran, M.; George, J.; Qian, X.-D.; Keilhauer, G.; Romerdahl, C. A. Preclinical Evaluation of LU79553: a Novel Bis-naphthalimide with Potent Antitumor Activity. *Cancer Res.* **1995**, *55*, 1176−1180.

(3) Braña, M. F.; Cacho, M.; García, M. A.; de Pascual-Teresa, B.; Ramos, A.; Acero, N.; Llinares, F.; Muñoz-Mingarro, D.; Abradelo, C.; Rey-Stolle, M. F.; Yuste, M. Synthesis, Antitumor Activity, Molecular Modelling and DNA Binding Properties of a New Series of Imidazonaphthalimides. *J. Med. Chem.* **2002**, *45*, 5813−5816.

(4) Braña, M. F.; Cacho, M.; Ramos, A.; Dominguez, M. T.; Pozuelo, J. M.; Abradelo, C.; Rey-Stolle, M. F.; Yuste, M.; Carrasco, C.; Bailly, C. Synthesis, Biological Evaluation and DNA Binding Properties of Novel Mono and Bisnaphthalimides. *Org. Biomol. Chem.* **2003**, *1*, 648−654.

(5) Patten, A. D.; Pacofsky, G.; Seitz, S. P.; Akamike, E. A.; Cherney, R. J.; Kaltenbach, R. F.; Orwat, M. J. Polycyclic and Heterocyclic Chromophores for Bis-imide Tumoricidals. Patent WO 9500490, 1995.

(6) Bailly, C.; Carrasco, C.; Joubert, A.; Bal, C.; Wattez, N.; Hildebrand, M.-P.; Lansiaux, A.; Colson, P.; Houssier, C.; Cacho, M.; Ramos, A.; Braña, M. F. Chromophore-modified Bis-naphthalimides: DNA Recognition, Topoisomerase Inhibition and Cytotoxic Properties of Two Mono- and Bis-furonaphthalimides. *Biochemistry* **2003**, *42*, 4136−4150.

(7) Deady, L. W.; Desneves, J.; Kaye, A. J.; Finlay, G. J.; Baguley, B. C.; Denny, W. A. Synthesis and Antitumor Activity of Some Indeno[1,2-*b*]quinoline-based Bis-carboxamides. *Bioorg. Med. Chem.* **2000**, *8*, 977−984.

(8) Gamage, S. A.; Spicer, J. A.; Finlay, G. J.; Stewart, A. J.; Charlton, P.; Baguley, B. C.; Denny, W. A. Dicationic Bis(9-methylphenazine-1-carboxamides): Relationships between Biological Activity and Linker Chain Stucture for a Series of Potent Topoisomerase Targeted Anticancer Drugs. *J. Med. Chem.* **2001**, *44*, 1407−1415.

(9) Braña, M. F.; Castellano, J. M.; Morán, M.; Pérez de Vega, M. J.; Perron, D.; Conlon, D.; Bousquet, P. F.; Romerdahl, C. A.; Robinson, S. P. Bis-naphthalimides 3: Synthesis and Antitumor Activity of *N*,*N*′-Bis[2-(1,8-naphthalimido)ethyl]alkanediamines. *Anti-Cancer Drug Des.* **1996**, *11*, 297−309.

(10) Gallego, J.; Reid, B. R. Solution Structure and Dynamics of a Complex Between DNA and the Antitumor Bisnaphthalimide LU-79553: Intercalated Ring Flipping on the Millisecond Time Scale. *Biochemistry* **1999**, *38*, 15104−15114.

(11) de Pascual-Teresa, B.; Gallego, J.; Ortiz, A. R.; Gago, F. Molecular Dynamics Simulations of the Bis-Intercalated Complexes of Ditercalinium and Flexi-Di with the Hexanucleotide $d(GCGCGC)_2$: Theoretical Analysis of the Interaction and Rationale for the Sequence Binding Specificity. *J. Med. Chem.* **1996**, *39*, 4810−4824.

(12) Braña, M. F.; Casarrubios, C.; Domínguez, G.; Fernández, C.; Pérez, J. M.; Quiroga, A. G.; Navarro-Ranninger, C.; de Pascual-Teresa, B. Synthesis, Cytotoxic Activities and Proposed Mode of Binding of a Series of Bis{[(9-oxo-9,10-dihydroacridine-4-carbonyl)amino]alkyl}alkylamines. *Eur. J. Med. Chem.* **2002**, *37*, 301−313.

(13) Bailly, C.; Braña, M.; Waring, J. Sequence-selective Intercalation of Antitumor Bis-naphthalimides into DNA. Evidence for an Approach Via the Major Groove. *Eur. J. Biochem.* **1996**, *240*, 195−208.

(14) Young, M. A.; Beveridge, D. L. Molecular Dynamics Simulations of an Oligonucleotide Duplex with Adenine Tracts Phased by a Full Helix Turn. *J. Mol. Biol.* **1998**, *281*, 675−687.

(15) Sherer, E. C.; Harris, S. A.; Soliva, R.; Orozco, M.; Laughton, C. A. Molecular Dynamics Studies of DNA A-Tract Structure and Flexibility. *J. Am. Chem. Soc.* **1999**, *121*, 5981−5991.

(16) Sprous, D.; Young, M. A.; Beveridge, D. L. Molecular Dynamics Studies of Axis Bending in $d(G5\ (GA4T4C)_2{-}C5)$ and $d(G5\text{-}(GT4A4C)_2{-}C5)$: Effects of Sequence Polarity on DNA Curvature. *J. Mol. Biol.* **1999**, *285*, 1623−1632.

(17) Pastor, N.; Pardo, L.; Weinstein, H. Does TATA Matter? A Structural Exploration of the Selectivity Determinants in its Complexes with TATA Box-binding Protein. *Biophys. J.* **1997**, *73*, 640−652.

(18) Cheatham, T. E. r.; Kollman, P. A. Observation of the A-DNA to B-DNA Transition During Unrestrained Molecular Dynamics in Aqueous Solution. *J. Mol. Biol.* **1996**, *259*, 434−444.

(19) Garcia-Nieto, R.; Manzanares, I.; Cuevas, C.; Gago, F. Bending of DNA upon Binding of Ecteinascidin 743 and Phthalascidin 650 Studied by Unrestrained Molecular Dynamics Simulations. *J. Am. Chem. Soc.* **2000**, *122*, 7172−7182.

(20) Cory, M.; Mckee, D. D.; Kagan, J.; Henry, D. W.; Miller, J. A. Design, Synthesis, and DNA Binding Properties of Bifunctional Intercalators. Comparison of Polymethylene and Diphenyl Ether Chains Connecting Phenanthridine. *J. Am. Chem. Soc.* **1985**, *107*, 2528−2536.

(21) Cohen, G.; Eisenberg, H. Deoxyribonucleate Solutions: Sedimentation in a Density Gradient, Partial Specific Volumes, Density and Refractive Index Increments, and Preferential Interactions. *Biopolymers* **1968**, *6*, 1077−1100.

(22) Wakelin, L. P. G. Polyfunctional DNA Intercalating Agents. *Med. Res. Rev.* **1986**, *6*, 275−340.

(23) Moinet-Hedin, V.; Tabka, T.; Poulain, L.; Godard, T.; Lechevrel, M.; Saturnino, C.; Lancelot, J. C.; Le Talaër, J. Y.; Gauduchon, P. Biological Properties of 5,11-Dimethyl-6*H*-pyrido[3,2-*b*]carbazoles: A New Class of Potent Antitumor Drugs. *Anti-Cancer Drug Des.* **2000**, *15*, 109−118.

(24) Sheehan, J. C.; O'Neill, R. C. The Formation of Five and Six-membered Rings by the Acyloin Condensation. II. The Cyclization of Dimethyl Hexahydrohomophthalate. *J. Am. Chem. Soc.* **1950**, *72*, 4614−4616.

(25) El-Rayyes, N. R.; Ali, A. H. A. The Stobbe Condensation with Dimethyl Homophthalate II. *J. Heterocycl. Chem.* **1976**, *13*, 83−88.

(26) Eigner, J.; Doty, P. The Native, Denatured and Renatured States of Deoxyribonucleic Acid. *J. Mol. Biol.* **1965**, *12*, 549−580.

(27) Müller, W.; Crothers, D. M.; Ihara, T. Interactions of Heteroaromatic Compounds with Nucleic Acids. 1. Influence of Heteroatoms and Polarizability on the Base Specificity of Intercalating Ligands. *Eur. J. Biochem.* **1975**, *54*, 267−277.

JM0308850